JOURNAL OF TECHNIQUES

Journal homepage: http://journal.mtu.edu.iq

RESEARCH ARTICLE - ENGINEERING

The Impact of (DEM) Accuracy and (LC/LU) Resolution on the Watersheds Areas

Alaa Qays Mutar[1*], Mustafa Tariq Mustafa[1], Muntasir Abdl Hameed Abdl Shareef[2]

[1] Engineering Technical College - Baghdad, Middle Technical University, Baghdad, Iraq.

[2] Institute of Technology – Baghdad, Middle Technical University, Baghdad, Iraq.

[*] Corresponding author E-mail: alaa.geo12@gmail.com

Article Info.

Article history:

Received
06 December 2021

Accepted
02 January 2022

Publishing
31 March 2022

Abstract

Land Cover/Land Use (LC/LU) and Digital Elevation Model (DEM) are the main inputs for watershed modelling. Recently, (DEM) and (LC/LU) are freely available as online open-source products in varied accuracies, spatial and spectral resolutions as result of several remote sensing platforms. Therefore, it is very important to determine which one is the optimum for modeling the watersheds in the selected study area, which is represented by five valley watersheds of diverse characteristics, located on east and west sides of the Mosul dam reservoir, Nineveh province, Iraq. In this research, the different accuracy of 30m resolution DEMs with Satellites (Copernicus (GLO-30), ASTER, and SRTM), besides to supervised classification (Support vector machines (SVM) classifier) results (LC/LU) main layers (green land, bare soil, urban areas, and water) of different spatial and spectral resolutions images with Satellites (10m Sentinel-2, 30m Landsat-8, and resampled 15m from 30m Landsat-8) are examined by using the techniques of Remote Sensing (RS) and Geographic Information System (GIS). Analysis of the results led to the finding that Copernicus DEM (GLO-30) 30 m spatial resolution is the most accurate and optimum DEM in the research study area with 1.1615 m vertical accuracy and 2.276 m at 95% confidence level. The optimum most accurate image for (LC/LU) thematic map production in the selected area is (Sentinel-2 l0 m) satellite at overall Classification accuracy (97%) and the overall kappa statistics (95%). The optimum remote sensing data (sentinel-2 image and Copernicus DEM) are mapped, 3D simulated and analyzed by GIS to calculate the areas of (LC/LU) main layers and to find that the considerable part of the selected watersheds is the area of green lands 404.32676 km^2 was about 54.396% of the total area in the study, and these areas are vary depending on many factors such as remote sensing data, precipitation, cultivation, season, and human activities.

This is an open access article under the CC BY 4.0 license (http://creativecommons.org/licenses/by/4.0/)

2019 Middle Technical University. All rights reserved

Keywords: Land Cover/Land Use; Watershed Delineation; Remote Sensing Satellites; Geographic Information System; Digital Elevation Model.

1. Introduction

A watershed is a landform - similar to a basin distinct by ridgelines and high elevation points that descent toward lower elevations and stream valleys. A watershed, in further terms, is a topographical region that contains a common group of streams and rivers that flow into main and more extensive body of water, for example an ocean, a larger river, or a lake. Shape, size, and vegetation, as examples in watershed, are substantial variables that affect in many aspects of runoff. In addition to Hydrological modeling, water resource management normally requires investigation of landscape, watershed boundary delineation, and hydrological features [1].

The quality (resolution and accuracy) of main input Remote Sensing (RS) data is essential for delineating the watersheds and forming the hydrologic simulation model. For example, the Land Cover/Land Use (LC/LU) map and the Digital Elevation Model (DEM) may affect the simulation results [2].

Some factors influence the selection of DEM resolution. Examples are cost, simulation time with reason, accessibility, and user requirements, among others [3]. In addition, several factors influence the DEMs vertical accuracy, such as the relief and roughness of the topography and the kind of vegetation [4].

Nomenclature & Symbols			
ASTER	Advanced Space-borne Thermal Emission and Reflection Radiometer	OLI	Operational Land Imager
BOA	Bottom-Of-Atmosphere	SRTM	Shuttle Radar Topography Mission
DEM	Digital Elevation Model	SVM	Support Vector Machines
EGM	Earth Gravitational Model	RMSE	Root Mean Square Error
GIS	Geographic Information System	RS	Remote Sensing
LC/LU	Land Cover/ Land Use	USGS	United States Geological Survey
LiDAR	Light Detection and Ranging	UTM	Universal Transverse Mercator
MOWR	Ministry of Water Resources	WGS84	World Geodetic System 1984
NASA	National Aeronautics and Space Administration	NGA	National Geospatial-Intelligence Agency

The most popular method for mapping land cover (LC) is digital image classification, which is described as "the process of producing thematic maps from images" [5].
The accuracy of classification does not always improve when the spatial resolution is increased. The increment in spatial resolution may reduce the class spectral separability, leading to a rise in classification errors. Some studies deal with the influence of spatial resolutions on classification accuracy. However, it is challenging to comprehensively understand the trade-off between the spatial resolution and classification accuracy [6]. It is critical to assess the impact of using various resolutions and origins of (DEM) and (LC/LU) for each watershed with varying topographic characteristics [7].

1.1. Problem Statement

Several studies use the data of satellite (images, DEM) with certain spatial and spectral resolutions to definite the region of watershed and delineate it, then extract (LC/LU) classes by classification methods to produce thematic maps for any watershed area. Most hydrological models use input data such as topography, Land Cover-Land Use (LC/LU). These data become accessible as products of several satellites in diverse accuracies, resolutions and sources. Therefore, it is essential to realize the influence of employing the satellite data from varied sources and resolutions in watersheds with a variety of topographic characteristics.
The diversity of, spatial, spectral resolutions and the source for the satellites data raises some questions:

1. What are the special effects of employing the highest accessible open-source DEM with not resampled resolution (original resolution), several accuracies in addition to sources, have on watershed delineation in the study area and what is the optimum freely available online satellite DEM study area?
2. What are the effects of different spatial, and spectral resolutions for online satellite images on (LC/LU) main classes (green land, bare soil, urban areas, and water) of different watersheds and what is the optimum, freely available online satellite image in study area?

1.2. Objectives of the Study

The main targets of this research are:
1. Examine the influences of using various input sources of the highest original resolution free (DEM) to delineate the watersheds with different sizes and topography.
2. Evaluate the effects of using different sources and spatial free input (images) to produce (LC/LU) thematic maps for main types (green land, bare soil, urban areas, and water) by using pixel-based supervised classification method through employing the Support Vector Machines classifier.
3. Specify the best free satellite data (DEM, images) for selected watersheds and calculate the areas of the mainland covers (green land, bare soil, urban areas, and water) of watersheds within study area to be provided for water resources experts to use the unit hydrograph approach to calculate the water runoff discharge for these areas.

1.3. Study Area Description

The study area is represented by five valleys watersheds of wide-ranging characteristics covers an area of approximately 742km2. Swaidy, Garlond, Khuwayr-Hirah valleys are positioned on the west side of Mosul reservoir, while Naqab and Kalak valleys are positioned at the east of reservoir. All these watersheds variate in topography, LC/LU regions and size. The water in the reservoir is from the Tigris river. In addition, the study area includes ten valleys, seven are on the east side, and the other three are on the west of the reservoir [8].
The selected study area northwest of Iraq extends between latitude 36°38'0" and 37°5'0" north and between longitude 42°5'0" and 42°52'0" east. These five valleys watersheds located on east and west sides of the Mosul dam reservoir which is about 60 km north of Mosul City, Nineveh province- Iraq, as shown in Fig. 1.
On the west side of Mosul dam reservoir, the main topography is fluctuated from a low rate of slope with a flat arable zone for a Swaidy valley that extents to Syrian Qarachock Mountain. While the Garlond valley is fluctuated from smooth to rugged areas, as for the Khuwayr Hirah valley, which is positioned in a rough hilly area extended to Jamrok Mountain, a big part of it is not suitable for agriculture.
The study area part in East side of the reservoir is within Duhok province, with an extensive variance in elevation. The Naqab and Kalak valleys start with undulant, rugged surface nearby the lake, afterwards increasingly change to flat arable topography and reach to mountainous zones in Bekher mountain. The maximum level among these five watersheds valleys extended (1346) m above sea level in Naqab Valley, and the lowest level (315) m at the outlet of Kalak valley. The recharge study area shows important seasonal periodic variations in precipitation, temperature and humidity characterized by wet winters and dry summers [9].
A substantial percentage of the research study area is covered by seasonal crops (barley and wheat), meadows and vegetables. [10].
The climate is similar to that of the Mediterranean, with certain differences due to Turkey's mountainous terrain. Winters are cold and rainy, with snowfall falling on rare occasions in mountainous regions, while summers are hot and dry. The rain season starts in the month of October and lasts until the month of May. [11], where annual rainfall over the Mosul dam site is (200- 600) mm [12].

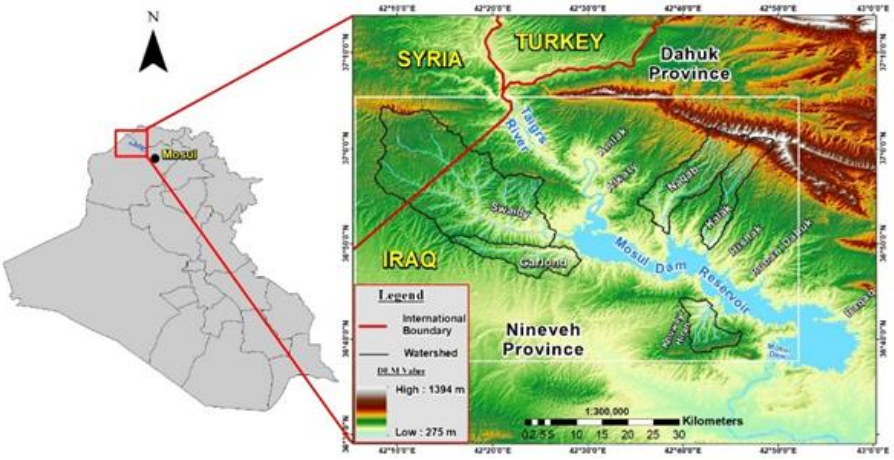

Fig 1. Study Area Location

2. Materials and Methods

The following sections explain the data, software used, and methods which used in this study.

2.1. Data description

The remote sensing data types used in this study can be depicted for the following:

- Watersheds delineation base on three satellite (DEMs) with a matching spatial resolution of 30 m. However, the data varies in accuracy level and production methods.
  Due to the availability of open source free DEMs on the internet with various spatial resolutions, accuracies, sources, and production methods, this variation led to the uneven representation of the topographic surface, affecting watershed delineation. Choosing the best accurate DEM for watershed delineation and other calculations in the study area becomes necessary.
  The choice for (30) m DEM spatial resolution was based on the fact that this resolution is the highest original resolution (not resampled) for the study area among known free DEMs websites.
  To select the best accurate DEM for the study area, three DEMs with the spatial resolution of 30m and of various vertical accuracy levels, sources, and production methods were tested as shown in Table 1. The accuracy of any DEM is affected by factors, such as the resolution (grid size) of the DEM. Hence, the quality of the source data, interpolation model, and degree of terrain complexity [13], with different LC/LU classes [14].
- For selecting and checking the most precise DEM for the research study area, (80) high accuracy points were employed, ((20) ground control points (GCPs) obtained by the fieldwork of the Iraqi ministry of water resources (MOWR), and (60) elevation points (checkpoints) covering parts of the study area extracted from high accuracy LiDAR DEM (1 m horizontal resolution, 0.2 m vertical resolution with heights from ellipsoid WGS84).
- The main LC/LU layers are derived from the images using supervised classification method on two satellite images. Different spatial and spectral resolutions, slight cloud cover over the study area, and slight difference in Acquisition Date for the two photos listed in Table 2 were downloaded and used to product main LC/LU classes in the study area.

The selection of images with different resolutions (spectral and spatial) because of the critical role these resolutions in classification results which were represented by the (LC/LU) classes [15]. Also, the accuracy of classification did not always improve when the spatial resolution was increased. The increase in spatial resolution caused the reduction of the class spectral separability, which led to an increment in classification errors. Despite many attempts, it remained unclear the influence of spatial resolutions on classification accuracy [6],[16].

Table 1 The main specifications of different downloaded satellites DEMs used in watershed delineation

	Tan DEM-X Copernicus (GLO-30)	(SRTM V3)	ASTER (GDEM V003)
Release year	2021 (for free)	2013	2019
Distribution	DLR - Airbus	USGS - NASA	METI - NASA
Data source	Tan DEM-X satellite	Space shuttle radar	ASTER Satellite
Production process	radar satellite SAR Interferometry	X-band with C-band SAR Interferometry	VNIR nadir with backward viewing telescopes
Spatial Resolution	30m	30m	30m
Data acquisition period	2011-2014	11 days in 2000	2000 to 2013
Vertical Absolute accuracy (RMSE)	4m (90% confidence)	16m (90% confidence)	20m (95% confidence)
Vertical reference	(EGM08)	(EGM96)	(EGM96)
Horizontal reference	(WGS84)	(WGS84)	(WGS84)

Table 2 Specifications of downloaded satellites images

Satellite	Landsat 8	Landsat 8	Sentinel-2
Acquisition Date	2020/05/08	2020/05/08	2020/05/14
Sensor Identifier	OLI	OLI_TIRS	MSI
bands	7	11	13
Processing level	C1 level-2	L1TP	2A
Atmospheric correction	Surface Reflectance (SR)	No	Bottom-Of-Atmosphere (BOA)
Geometric correction	yes	yes	yes
Spatial Resolution	30 m	15 m	30 m
for used bands	Bands (1, 2, 3, 4, 5, 6, 7, 9)	Band (8)	Bands (1, 2, 3, 4, 5, 6, 7, 9)
Map Projection	UTM	UTM	UTM
UTM Zone	38	38	38
Ellipsoid	WGS84	WGS84	WGS84
Datum	WGS84	WGS84	WGS84

2.2. The Software Used

Various software is required to achieve the research objectives. However, for this task, three computer software packages were utilized:

- ArcGIS 10.8 used for many aspects of this study such as, data preparation, watersheds delineation, create maps, perform spatial analysis, with manage geographic data and results verification.
- ERDAS IMAGINE 14 used to process relevant images via remote sensing and image analysis methods.
- ENVI 5.3 is used for visualizing, spectral image processing, and image analysis. Also, it is important to mention that this software is tightly integrated with Esri's ArcGIS software.

2.3. Methodology of the Research

The complete research can be divided into some phases. The overview diagram of research mythology is shown in Fig. 2.

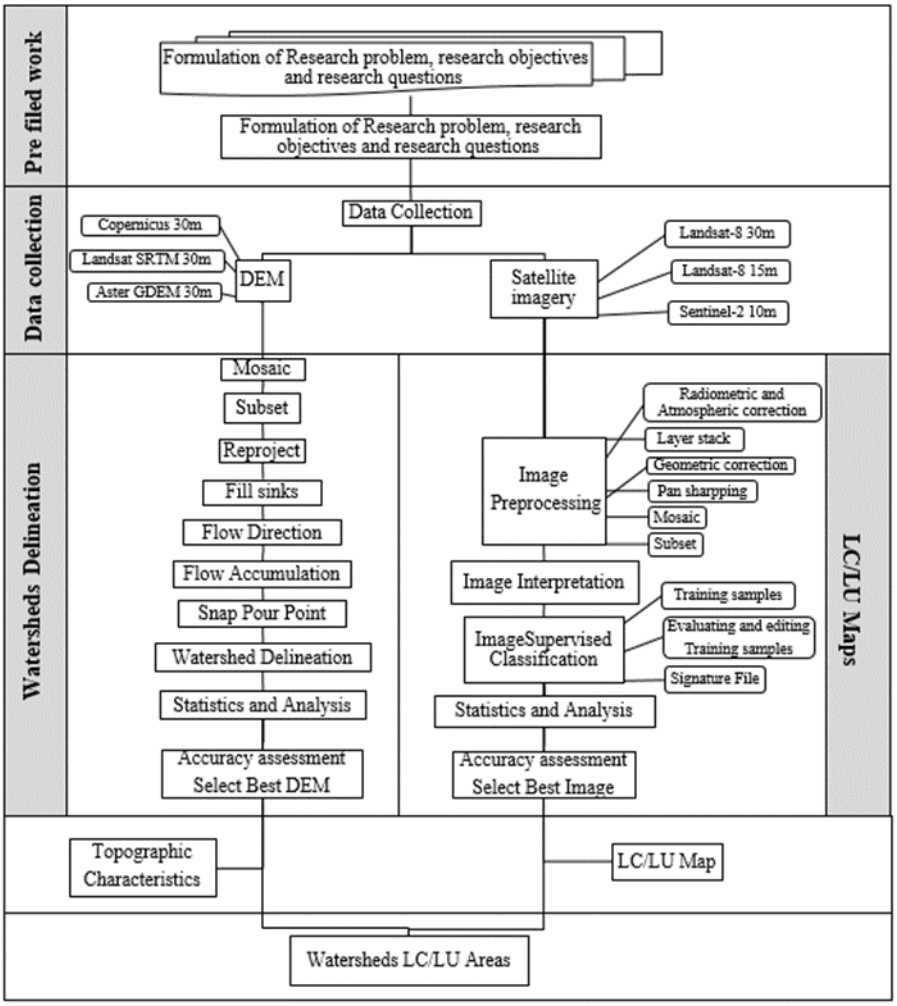

Fig 2. Flowchart of the research

2.4. Watershed Delineation

The delineation of watersheds was performed by using DEM data (SRTM DEM 30 m, Copernicus DEM 30 m and GDEM 30 m) for several phases which were required to convert the DEM data to flow direction with accumulation data, then lastly into delineated watersheds. The definite tools which needed for delineate the watersheds were found in the Hydrology tools within the Spatial Analyst toolbox extension in software (ArcGIS Desktop 10.8), Pour points, flow direction, and flow accumulation are all taken into account in this process as shown in Fig. 3 to 5.

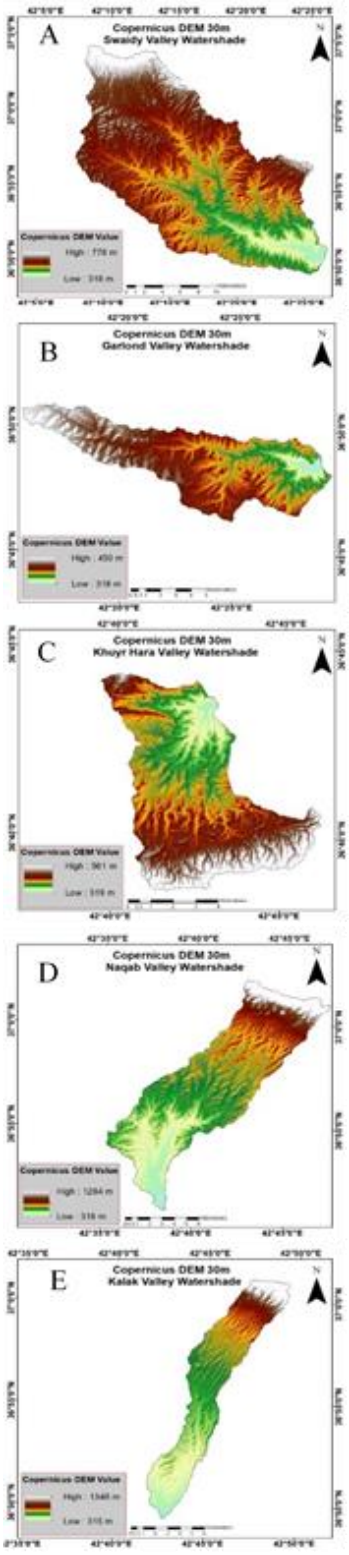

Fig 3. Delineated watersheds by Copernicus DEM (30) m

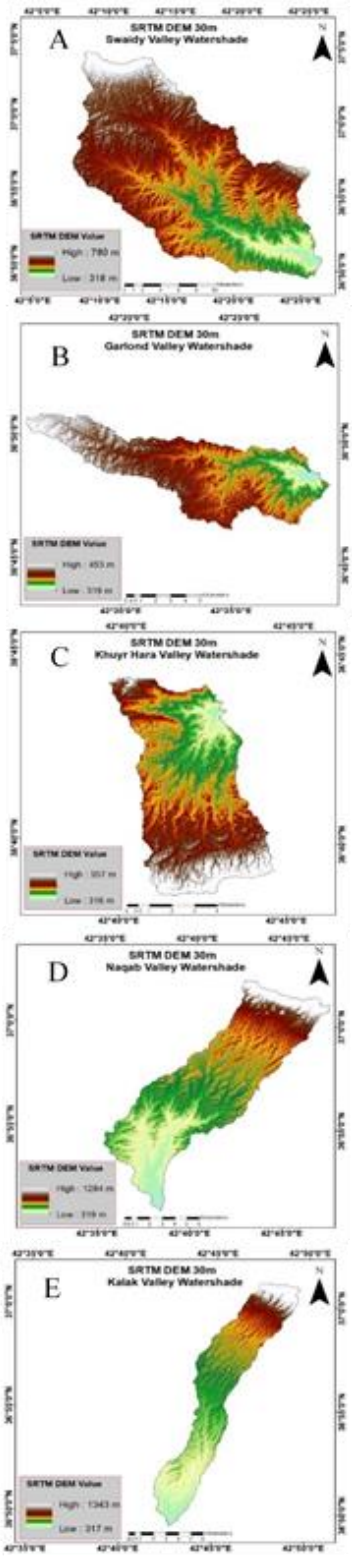

Fig 4. Delineated watersheds by SRTM DEM (30) m

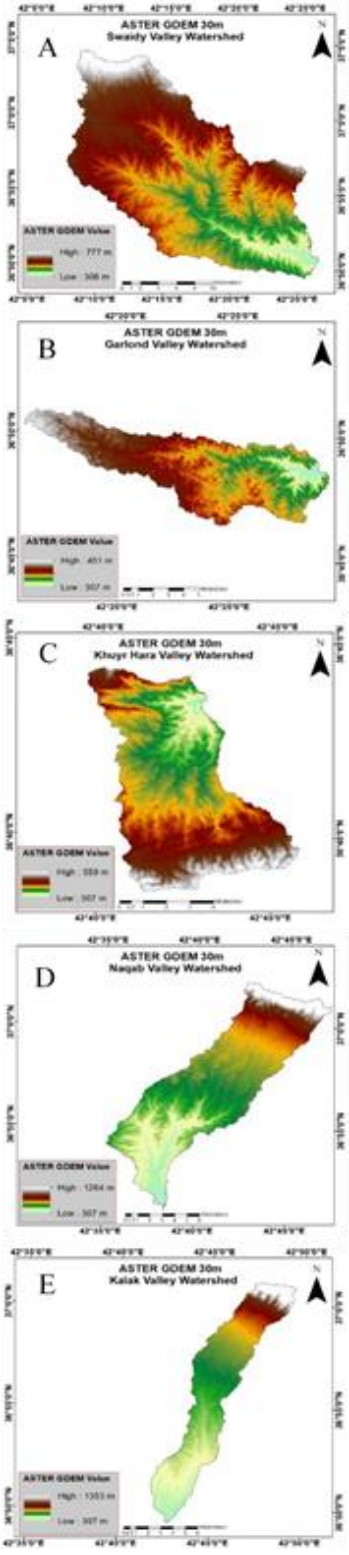

Fig 5. Delineated watersheds by ASTER GDEM (30) m

2.5. LC/LU MAP

The most commonly used technique for mapping LU/LC is image classification which done by using (ArcGIS Desktop 10.8) software. The first phase in image classification may be to choose a suitable classification method.
The use of remote sensing datasets to classify watershed regions is essential for hydrological modeling and/or a better understanding of runoff processes [17].
Because the accuracy of classification did not always improve when the spatial resolution was increased [6]. For this study, more than one spectral and spatial resolution satellite image was employed as follows:

- Landsat-8 low spatial resolution of (30) m and fused image of (15) m between the images that have a (30) m resolution with the high-resolution PAN image of (15) m can be adopted by spectral sharpening algorithm.
- Sentinel satellite imagery of (10) m is adopted to execute the pre-processing besides processing operations and then pixel-based supervised classification.

Based on the kind, processing level and the reason that the downloaded satellite images will be used, the preprocessing operations done on these downloaded satellite images are: Geometric correction, Radiometric Calibration, Atmospheric Correction, Layer stack, Pan sharping, Mosaic and Subset.
In order to improve multispectral images classification results in supervised classification method for the study area, the general image visual analysis and interpretation were relied upon, besides the information was gathered about topography, features, LC\LU for the study area in all different downloaded spectral and spatial resolutions images.
The Images interpretation Process is essential because in image supervised classification, the selecting sample pixels to represent the specific right land cover depend on the user expertise and correct image interpretation for all features and LC/LU in the study area.

2.6. Images Supervised Classification

The most common image analysis method used for medium and low-resolution images is a pixel-based classification, where objects of interest in images are smaller than, or nearly equal to, the image pixel size [18].
The selection of a classification method depends on some factors like the type of resources, type of application, and data available [19]. So, this study uses the pixel-based supervised classification method by employing the statistical learning-based classifier (non-parametric rule of Support Vector Machines).
This choice is based on many studies that have discovered that Support Vector Machines (SVM) achieves higher accuracy than other classification algorithms such as Maximum Likelihood Classification (MLC) [20-22].
The (ArcGIS 10.8) software is used based on the spectral differences between different classes in the image. These differences are employed to subdivide the study area's main LC/LU classes into separate classes (green, bare soil, urban and water).

3. Results and Discussion

3.1. Optimum DEM for the research study area

For selecting and checking the most precise DEM for this research study area, (80) precise elevation check points were employed, ((20) control points from fieldwork of Iraqi (MOWR) which collected in September-2020 in Mosul dam by employing (Topcon Gr5 Gnss Receiver and Topcon GPT-7501 total station), with (60) point was extracted from LIDAR DEM (0.2 m vertical accuracy, 1m horizontal resolution with altitudes from WGS48 ellipsoid) cover portions of study area).
Choosing the most precise DEM was made by matching the (80) checkpoints elevations with extracted elevations from DEMs used to delineate the watersheds (SRTM, Copernicus DEM and Aster GDEM) for the same point (same E/N coordinates) after all these elevations were unified to (EGM96) by converting the vertical reference of Copernicus DEM from (EGM08) to (EGM96) using (ERDAS IMAGINE 14) software.
Based on the resulted elevation differences which shown in Fig. 6, the Root Mean Square Error (RMSE) and at 95% confidence level RMSE are computed for the resulted differences as shown in Table 3.

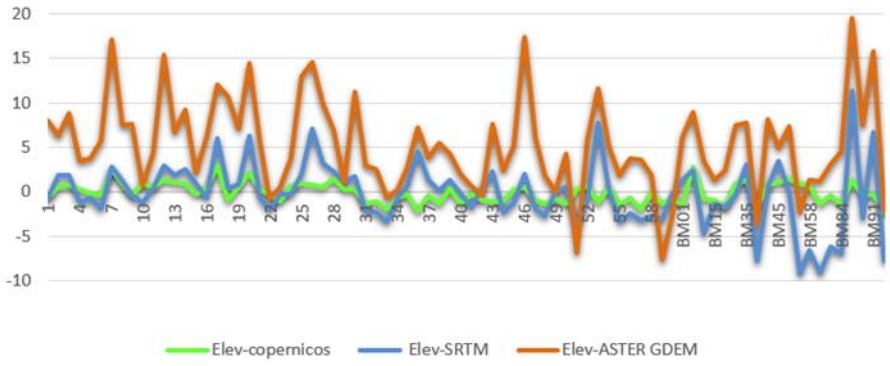

Fig 6. The difference in elevations between used checkpoints and DEMs

Table 3 The RMSE results for the difference in elevations between used checkpoints and DEMs

	Copernicus	SRTM	ASTER DEM
R.M.S.E (m)	1.352	3.599	7.049
95% confidence level R.M.S.E (m)	2.650	7.053	13.816

Relaying on the analysis of results, the Copernicus DEM has least RMSE ith 95% confidence level RMSE, which suggests vertical accuracy more than the other used DEMs in the research study area (Landsat SRTM and Aster GDEM), respectively. These findings are in line with the studies of [23-24], besides the vertical accuracy specifications of used DEMs as shown in Table 4. which extracted from Table 1.

Table 4 Vertical accuracy specifications of used DEMs

	Copernicus (GLO-30)	(SRTM V3)	ASTER (GDEM V003)
Vertical absolute accuracy (RMSE)	4 m (90% confidence level)	16 m (90% confidence level)	20 m (95% confidence level)

As a result, in the selected study area, the Copernicus DEM is the best DEM for watershed delineation and other topographic calculations.

3.2. Optimum Images for supervised classification in the selected study area

In order to find the Optimum Images for supervised classification, the accuracy of images classification must be assessed. accurate reference data or ground truth is needed, therefore based on high-resolution imagery from base map ArcGIS online and Sentinel (10 m) resolution images, 250 selected points that are covered the features can be classified (green, bare land, urban and water) in all watersheds. These points are created on the satellite images by using (ArcGIS Desktop 10.8) software as shown in Fig. 7.

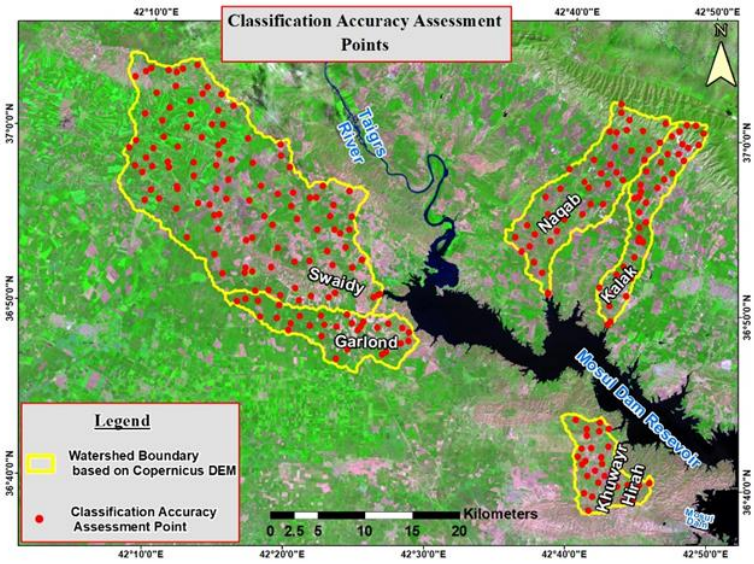

Fig 7. Location of assessment points of images Classification Accuracy

The overall accuracy and kappa coefficient for each satellite image (Landsat 8-30m and 15m, Sentinel 2-10m) in the area of interest is calculated by the Compute Confusion Matrix tool in ArcGIS tools box as shown in Fig. 8.

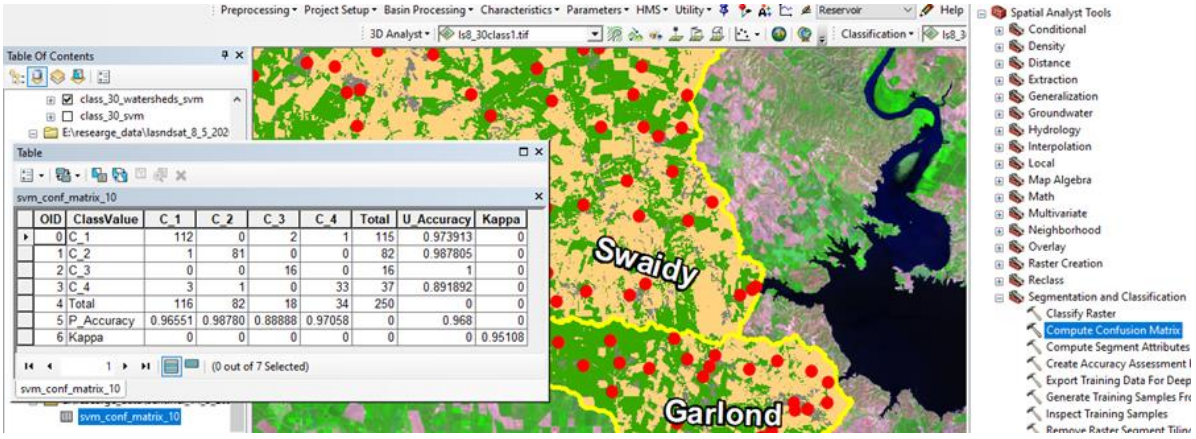

Fig 8. Accuracy assessment matrix of classification for sentinel (10 m image)

The comparison is made with classified images to assess the accuracy of classification as shown in Table 5.

Table 5 Accuracy assessment matrices of classification for used images

	class value	green	bare land	water	Urban	total	user's accuracy	kappa
sentinel2_10m	green	112	0	2	1	115	0.97391	0
	bare land	1	81	0	0	82	0.98781	0
	water	0	0	16	0	16	1	0
	urban	3	1	0	33	37	0.89189	0
	Total	116	82	18	34	250	0	0
	producer's accuracy	0.96552	0.98781	0.888899	0.97059	0	0.968	0
	Kappa	0	0	0	0	0	0	0.95109
	class value	green	bare land	water	Urban	total	user's accuracy	kappa
Landsat_15m	green	108	0	2	0	110	0.981818	0
	bare land	1	82	0	0	83	0.987952	0
	water	1	0	15	0	16	0.9375	0
	urban	6	2	1	32	41	0.780488	0
	Total	116	84	18	32	250	0	0
	producer's accuracy	0.93103	0.97619	0.83333	1	0	0.948	0
	Kappa	0	0	0	0	0	0	0.92106
	class value	green	bare land	water	Urban	total	user's accuracy	kappa
Landsat_30m	green	104	0	3	1	108	0.96296	0
	bare land	5	82	0	0	87	0.94253	0
	water	2	0	14	0	16	0.875	0
	urban	5	2	1	31	39	0.79487	0
	Total	116	84	18	32	250	0	0
	producer's accuracy	0.89655	0.97619	0.77778	0.96875	0	0.924	0
	Kappa	0	0	0	0	0	0	0.88451

The overall accuracy beside kappa coefficient for all used satellite images (Landsat 8-30 m and 15 m, Sentinel 2-10 m) in the area of interest from Table 5 is computed and listed in Table 6.

Table 6 Overall accuracy and kappa coefficient for each used satellite image

	Landsat 30m	Landsat 15m	Sentinel 10m
Overall Classification Accuracy	92%	95%	**97%**
Overall Kappa Statistics	88%	92%	**95%**

Therefore, the Classification for Sentinel 2 (10 m spatial resolution, covering 13 spectral bands and equation data in 14/5/2021) satellite image is the most accurate with the rest of the other used images (Landsat 8-30 m and 15 m).

3.3. (LC/LU) thematic maps production

The results of the classification with the optimum satellite image for (LC\LU) map production in the selected study area (Sentinel_2) is a raster content of four classified layers (green, bare soil, urban, and water) which represent the main LC/LU layers in the selected study area as shown in Fig. 9.

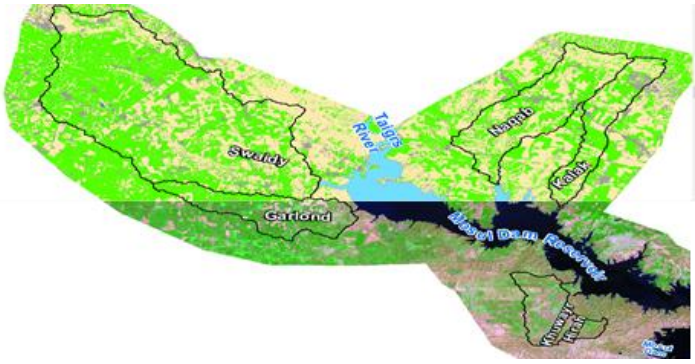

Fig 9. Produced raster of classified layers

The produced raster was cut out based on watersheds boundaries which delineated from the optimum DEM (Copernicus GLO30) in the study area, and the maps were produced by using (ArcGIS Desktop 10.8) software. Each watershed was simulated by using Arc Scene extension as shown in Fig. 10 to 14.

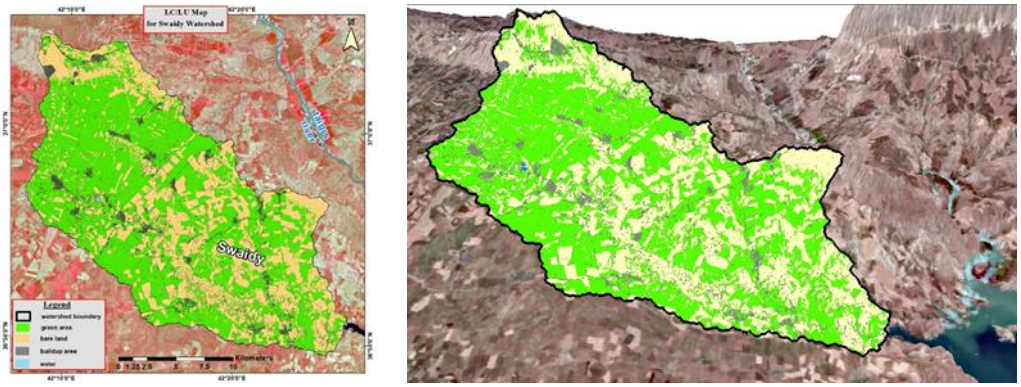

Fig 10. LC/LU Map and 3D simulation for Swaidy watershed of optimum remote sensing data (Sentinel-2 image and Copernicus DEM)

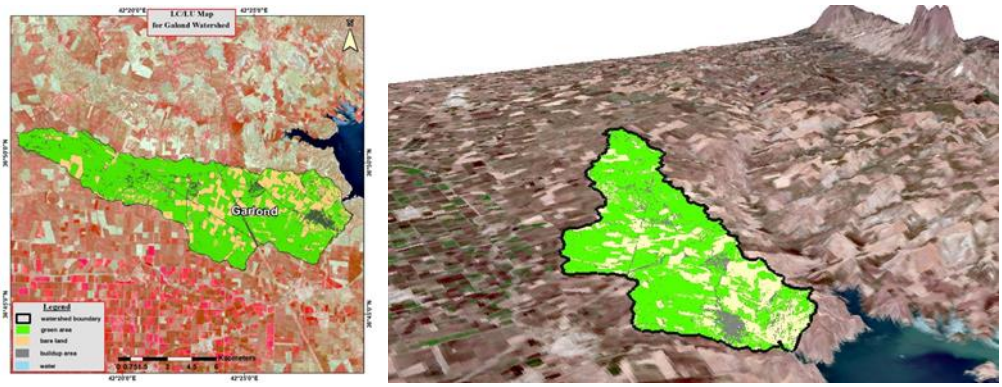

Fig 11. LC/LU Map and 3D simulation for Garlond watershed of optimum remote sensing data (Sentinel-2 image and Copernicus DEM)

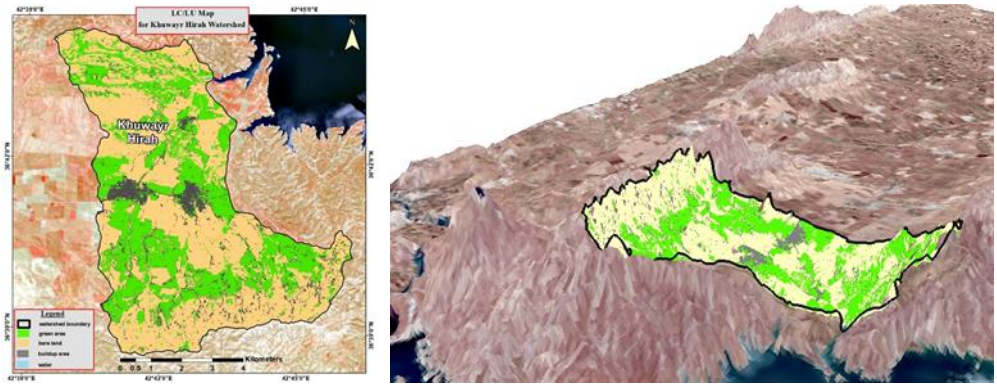

Fig 12. LC/LU Map and 3D simulation for Khuwayr Hirah watershed of optimum remote sensing data (Sentinel-2 image and Copernicus DEM)

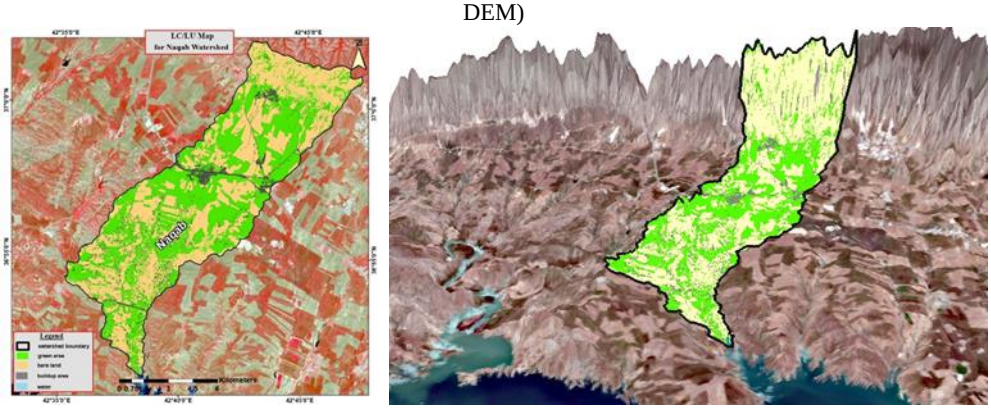

Fig 13. LC/LU Map and 3D simulation for Naqab watershed of optimum remote sensing data (Sentinel-2 image and Copernicus DEM)

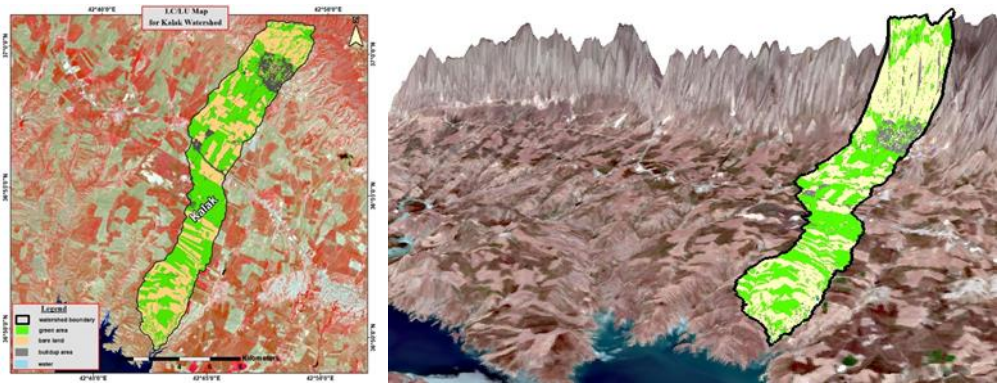

Fig 14. LC/LU Map and 3D simulation for Kalak watershed of optimum remote sensing data (Sentinel-2 image and Copernicus DEM)

3.4. LC/LU areas computations for each watershed

The area of each layer resulted from the supervised classification of the optimum image in this study area with (Sentinel 2 satellite image) for each delineated watershed concluded from the optimum DEM in this study area with (Copernicus DEM) can be computed. The (ArcGIS Desktop 10.8) software is employed to convert the produced raster from supervised classification to vector layers, then compute the areas of layers in (km2) for each watershed as shown in Table 7.

Table 7 The areas in (km^2) of classified layers for each watershed of optimum remote sensing data (Sentinel-2 image and Copernicus DEM)

Watershed / Class name	Swaidy	Garnold	Khuwar Hirah	Naqab	Kalak	all
green	244.36423	51.86498	18.18125	56.34450	33.57181	404.32676
bare land	147.01046	18.59708	29.55311	56.72932	29.21997	281.10994
urban	32.53356	6.45905	4.87201	7.84698	5.83756	57.54916
water	0.15585	0.02761	0.02139	0.05149	0.05893	0.31527
total areas	424.06410	76.94871	52.62776	120.97228	68.68828	743.30113

The percentage of the classified LC/LU layers areas for each watershed is shown as a pie chart in Fig. 15 and Table 8.

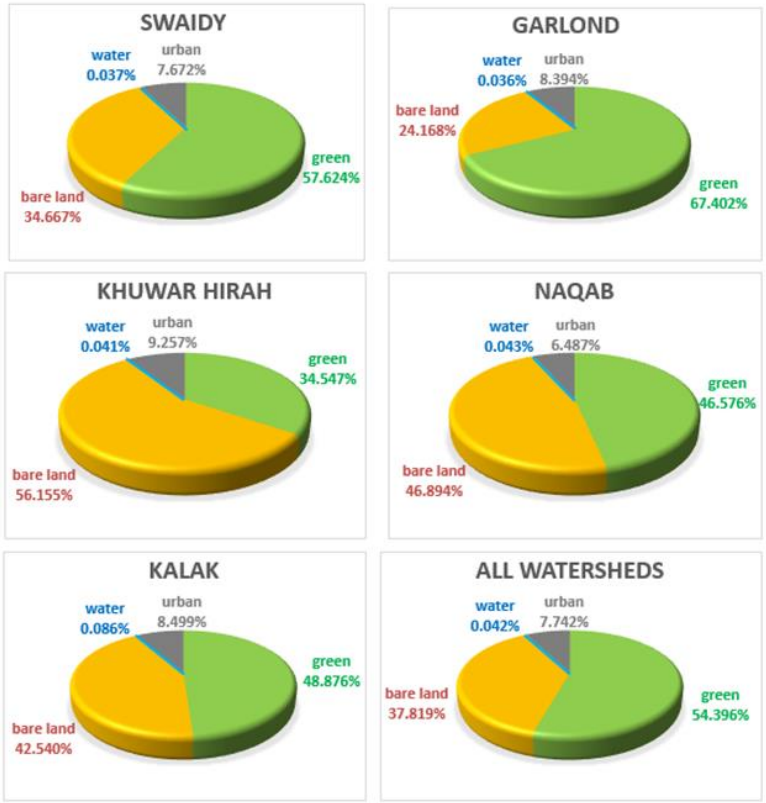

Fig 15. Pie chart of LC/LU layers areas percentage for each watershed of optimum remote sensing data (Sentinel-2 image and Copernicus DEM)

Table 8 The areas percentage (%) of classified layers for each watershed of optimum remote sensing data (Sentinel-2 image and Copernicus DEM)

Watershed / Class name	Swaidy	Garnold	Khuwar Hirah	Naqab	Kalak	all
green	57.62436	67.40201	34.54687	46.57637	48.87561	54.39609
bare soil	34.66704	24.16814	56.15499	46.89448	42.53997	37.81912
urban	7.67185	8.393969	9.257493	6.486592	8.498625	7.742375
water	0.036752	0.035878	0.040644	0.04256	0.085795	0.042414

From Tables 7 and 8, the green lands area represents the largest part with an area of 404.32676km2, a percentage of 54.4% of the watershed areas. These areas of classified layers change depending on factors such as precipitation, cultivation, season, and human activities. Results, shown in Fig. 16, reveal the difference in some of main LC/LU areas, such as green and bare soil, of the selected study area between the date of the classified satellite image (14/5/2020) and about three months later (12/8/2020).

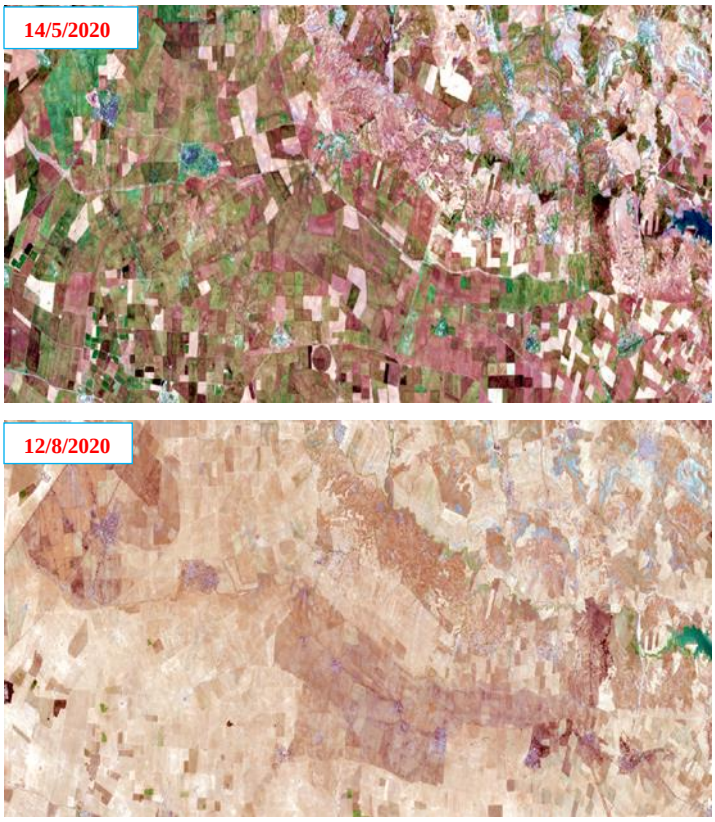

Fig 16. Comparison of a part of the study area between two dates

4. Conclusion

The following are the main critical conclusions that were obtained from analyses of the results in this study:

1. For the selected study area, the open source Copernicus (GLO-30) DEM is the optimum 30 m resolution DEM. The RMSE values for the differences in elevations between verification points (LiDAR DEM and MOWR GCPs) with the employed DEMs of the Copernicus (GLO-30) was (1.352 m) and (2.65 m) with 95% confidence level. Hence, it might be relied on the optimum DEM for delineate the watersheds and other topographic characteristics calculations, both the SRTM and ASTER DEMs respectively comes after the Copernicus DEM in accuracy respectively.
2. The optimum, accurate image for LC/LU thematic map production for the selected study area is with the sentinel 2-10m satellite at overall classification accuracy of 97% and the overall Kappa Statistics of 95%.
3. The considerable part of the selected watersheds area is the green lands of (404.364 km2) about (54.396 %) of the total area by using the optimum remote sensing data (sentinel-2 image and Copernicus DEM).
4. The areas of the main (LC/LU) in the study area (green, bare soil, urban and water) vary depending on many factors such as precipitation, cultivation, season, and human activities. So, in order to reach the highest possible accuracy in watersheds modeling the production of (LC/LU) layers must be based on a recent image as much as possible.

Acknowledgement

The authors are thankful to the MoWR (Ministry of Water Resources), Iraq, to accomplish this study. The authors also extend profound gratitude to the reviewers of this paper for their highly significant recommendation.

Reference

[1] R. Palaka and G. J. Sankar, "Study of watershed characteristics using Google Elevation Service," in Geospatial world, 2016, no. March, doi: 10.13140/2.1.5103.0080.
[2] J. Kim, J. Noh, K. Son, and I. Kim, "Impacts of GIS data quality on determination of runoff and suspended sediments in the Imha watershed in Korea," Geosci. J., vol. 16, no. 2, pp. 181–192, 2012, doi: 10.1007/s12303-012-0013-8.
[3] C. C. Mbajiorgu, K. N. Ogbu, and V. Ogwo, "IMPACT OF DEM RESOLUTION ON WATERSHED TOPOGRAPHIC INDICES AND SIMULATED HYDROLOGIC MODELING RESULTS," no. September, 2015.
[4] J. Thomas, V. Prasannakumar, and P. Vineetha, "Suitability of spaceborne digital elevation models of different scales in topographic analysis: an example from Kerala, India," Environ. Earth Sci., vol. 73, no. 3, pp. 1245–1263, 2015, doi: 10.1007/s12665-014-3478-0.
[5] R. A. Schowengerdt, Remote Sensing: Models and Methods for Image Processing, 3rd ed. Elsevier Inc., 2007.
[6] P. F. Hsieh, L. C. Lee, and N. Y. Chen, "Effect of spatial resolution on classification errors of pure and mixed pixels in remote sensing," IEEE Trans. Geosci. Remote Sens., vol. 39, no. 12, pp. 2657–2663, 2001, doi: 10.1109/36.975000.
[7] F. H. Saeed and M. S. Al-Khafaji, "Assessing the Accuracy of Runoff Modelling with Different Spectral and Spatial Resolution Data Using SWAT Model." Thesis submitted to the building and construction engineering Department, University of Technology, 2016.
[8] M. E. Mohammad, N. Al-Ansari, I. E. Issa, and S. Knutsson, "Sediment in Mosul Dam reservoir using the HEC-RAS model," Lakes Reserv. Res. Manag., vol. 21, no. 3, pp. 235–244, 2016, doi: 10.1111/lre.12142.
[9] IAMAT, "Iraq Climate Data," 24 world climate and food safety charts, 2020. https://www.iamat.org/country/iraq/climate-data (accessed Dec. 30, 2020).
[10] M. E. Mohammad, N. A. Al-Ansari, and S. Knutsson, "Sediment delivery from right bank valleys to Mosul Reservoir Iraq," J. Ecol. Environ. Sci., vol. 3, no. 1, pp. 50–53, 2012.
[11] N. Al-ansari and S. Knutsson, "Toward Prudent management of Water Resources in Iraq," J. Adv. Sci. Eng. Res., vol. 1, pp. 53–67, 2011.
[12] ECB, "Sedimentation study at the intake of North Al- Jazeera Irrigation project. Final report," Eng. Consult. Bur., p. 112, 2010.
[13] W. Shi, B. Wang, and Y. Tian, "Accuracy Analysis of Digital Elevation Model Relating to Spatial Resolution and Terrain Slope by Bilinear Interpolation," Math. Geosci., vol. 46, no. 4, pp. 445–481, 2014, doi: 10.1007/s11004-013-9508-8.
[14] W. Katerji, M. F. Abadia, and M. D. C. M. Balsera, "Dem Local Accuracy Patterns in Land-Use/Land-Cover Classification," Open Geosci., vol. 8, no. 1, pp. 760–770, 2016, doi: 10.1515/geo-2016-0052.
[15] C. Suwanprasit and N. Srichai, "Impacts of spatial resolution on land cover classification," Proc. Asia-Pacific Adv. Netw., vol. 33, no. 0, p. 39, 2012, doi: 10.7125/apan.33.4.
[16] Y. Yanjun, T. Qingjiu, Z. Yulin, T. Bo, and X. Kaijian, "Effects of Spatial Resolution and Texture Features on Multi-spectral Remote Sensing Classification," Geo-information Sci., vol. 20, no. 1, pp. 99–107, 2018, doi: 10.12082/dqxxkx.2018.170177.
[17] L. Chasmer, C. Hopkinson, T. Veness, W. Quinton, and J. Baltzer, "A decision-tree classi fi cation for low-lying complex land cover types within the zone of discontinuous permafrost," Remote Sens. Environ., vol. 143, pp. 73–84, 2014, doi: 10.1016/j.rse.2013.12.016.
[18] T. Blaschke, "Object based image analysis for remote sensing," ISPRS J. Photogramm. Remote Sens., vol. 65, no. 1, pp. 2–16, 2010, doi: 10.1016/j.isprsjprs.2009.06.004.
[19] N. Dey, A. S. Ashour, and C. Bhatt, Eds., Big Data for Remote Sensing: Visualization, Analysis and Interpretation. Springer, 2019.
[20] A. Razaque, M. Ben Haj Frej, M. Almi'ani, M. Alotaibi, and B. Alotaibi, "Improved support vector machine enabled radial basis function and linear variants for remote sensing image classification," Sensors, vol. 21, no. 13, pp. 1–26, 2021, doi: 10.3390/s21134431.
[21] B. Rimal, S. Rijal, and R. Kunwar, "Comparing Support Vector Machines and Maximum Likelihood Classifiers for Mapping of Urbanization," J. Indian Soc. Remote Sens., vol. 48, no. 1, pp. 71–79, 2020, doi: 10.1007/s12524-019-01056-9.
[22] A. Mondal, S. Kundu, S. K. Chandniha, R. Shukla, and P. K. Mishra, "Comparison of Support Vector Machine and Maximum Likelihood Classification Technique using Satellite Imagery," vol. 1, no. 2, pp. 116–123, 2012.
[23] C. H. Grohmann, "Evaluation of TanDEM-X DEMs on selected Brazilian sites: Comparison with SRTM, ASTER GDEM and ALOS AW3D30," Remote Sens. Environ., vol. 212, no. September 2017, pp. 121–133, 2018, doi: 10.1016/j.rse.2018.04.043.
[24] P. L. Guth and T. M. Geoffroy, "LiDAR point cloud and ICESat-2 evaluation of 1 second global digital elevation models: Copernicus wins," Trans. GIS, vol. 25, no. 5, pp. 2245–2261, 2021, doi: 10.1111/tgis.12825.